MICROSTRUCTURAL EVOLUTION OF LASER METAL DEPOSITED 17-4 PH SS-TUNGSTEN COMPOSITE WITH VARYING VOLUME PERCENT TUNGSTEN

A. A. Adeyemi[1], E.T. Akinlabi[1], R. M. Mahamood[1,2*]

[1]Department of Mechanical Engineering Science, University of Johannesburg, South Africa
[2]Department of Mechanical Engineering, University of Ilorin, Nigeria
*Corresponding author's e-mail address: mahamoodmr2009@gmail.com

ABSTRACT

This study investigates the influence of quantity of tungsten powder on the microstructural evolution of 17-4 PH stainless steel-tungsten composite produced using laser metal deposition process. The 17-4 PH stainless steel and tungsten powders were deposited on 316 stainless steel substrate at laser power of 2600 W. The tungsten powder flow rate was varied between 0.5 rpm and 2.0 rpm while 17-4 PH stainless steel powder flow rate, the scanning speed, the gas flow rate and the laser spot size were fixed at 2.0 rpm, 0.5 m/s, 2.5 l/min and 2.0 mm respectively. Five (5) multiple track of 17-4 PH stainless steel and tungsten powder were deposited on 316 stainless steel of thickness 10 mm from different hopper at 50% overlapping percentage to produce 17-4 PH SS-W composite. During the microstructural study, it was observed that tungsten carbide has been precipitated in-situ and evenly dispersed in the 17-4 PH SS-W composite produced. SEM and EDS analysis also revealed the presence of BCC alpha (α) ferrite and FCC gamma (δ) ferrite with the presence of sigma (σ) phase precipitates.

KEYWORDS: Laser Metal Deposition, Laser Power, Microstructure, Precipitation hardening stainless steel composite and Tungsten

1. INTRODUCTION

Precipitation hardening stainless steel (17-4 PH stainless steel) is an important engineering material that finds its application in a number of industries because of their outstanding properties that include high corrosion resistance, high hardness, high strength and high ductility.[1]. Industries that find 17-4 PH stainless steel useful include automobile industry, oil and gas industry (for pressure vessels), agriculture and mining industry [2]. 17-4 PH stainless steel is martensitic and in the matrix of face centred cubic (FCC) austenite structure. After solution heat treatment and during cooling of this alloy, the alloy exhibits two major microstructures, δ- ferrite (a body centred cubic lattice structure (BCC)) and austenite (a face centred cubic lattice structure (FCC)). As the alloy further cools down, some of the austenite (FCC) is transformed into martensite. The remaining alloy not transformed is referred to as retained austenite.

Typically, 17-4 PH stainless steel has dendritic microstructure which consists of 50% retained austenite and 50% martensite. Ageing is the process of further heating of the alloy after cooling to martensite state. The ageing temperature is between 450–510°C, when the precipitates of copper-rich clusters are formed which are responsible for the high strength and high hardness of 17- PH stainless steel alloy [2, 3].

Tungsten on the other hand is a refractory material that is used in high temperature applications [4]. Tungsten is an important metal with high melting point, high density with low coefficient of thermal expansion and excellent thermal conductivity property. These unique properties of tungsten make it find its application in industries such as aerospace, and automobiles industries. It is also used for industrial protector, radiation shielding, nuclear medicine, space vehicle equipment and as metal cutting tools materials [5]. Tungsten also finds it application in extreme working environment where high wear rate is dominant such as in rocket nozzles [6], steam turbines, high voltage electrical contacts and piercing plugs for seamless pipe production [5]- [7]. Tungsten is also used in combination with other materials such as metals and alloys to produce composite materials.

Composites materials offer unusual combination of mechanical properties such as high temperature resistance, high hardness and high wear resistance. The most commonly used fabrication process for metal matrix composites are powder metallurgy, spray deposition and squeeze casting. To extend the state of literature for the fabrication techniques of producing metal matrix composites, additive manufacturing has also been used as a modern fabrication technique to manufacture engineering materials with enhanced mechanical properties [8].

Additive manufacturing is an advanced manufacturing for producing complex shaped parts by adding materials layer by layer. Additive manufacturing technology includes selective laser sintering/melting, fused deposition modelling (FDM) and laser metal deposition (LMD) process [9-13]. The LMD process is an additive manufacturing process that is used to fabricate three dimensional (3D) parts in a layer wise manner by depositing materials according to the 3D computer aided design (CAD) data [14]. The LMD process is sensitive to processing parameters which include laser power, scanning speed, powder feed rate, gas flow rate and laser spot diameter. The process parameters have shown to have great influence on the properties of the parts produced and these process parameters need to be optimized for the required application [15-21]. Laser metal deposition has been extensively used with various engineering materials to fabricate metals, alloys and composites materials which include stainless steel, titanium alloys and aluminium alloys [8, 22-25].

The study of 17-4 PH stainless steel composite processed using LMD process is very scares in the literature. The 17-4 PH/tungsten composite is an important composite material for engineering application and understanding the evolving microstructure with varying percentage of tungsten will go a long way in designing a composite material for suitable application. In this study, tungsten powder at varying percentage achieved by changing the powder flow rate was deposited with 17-4 PH stainless steel using the LMD process to produce 17-4 PH SS-W composite. The resulting microstructure were studied and analysed.

2. EXPERIMENTAL METHOD

The materials used in this study are 17-4 PH stainless steel powder with chemical composition presented in table 1., tungsten powder and 316 stainless steel as substrate material. The average particle size of 17-4 PH stainless steel powder ranges between 45 µm and 90 µm while tungsten powder particle size ranges between 11 µm and 15 µm. The LMD process research was carried out using Ytterbium fibre laser system of maximum output power of 3000 W with laser wavelength of 1060 nm attached to kuka robotic arm which was used to achieve the LMD process. The laser beam was used to create melt pool on the surface of the substrate on which the metallic powders are introduced and melted. The two powders were placed in separate powder hopper and introduced into the melt pool through coaxial nozzles that are attached to the end effector of the Kuka robot. Multiple tracks at 50% overlapping percentage were produced which upon solidification form a solid metallic deposit in form of a composite. The LMD was carried out in the presence of argon gas at a flow rate of 2.5 l/min to prevent the melt pool from oxidizing thereby shielding it from oxygen and Nitrogen. Table 1 shows the elemental composition of the 17-4 PH stainless steel powder.

Before the deposition process, 17-4 PH stainless steel and tungsten metallic powder were placed in separate hoppers while the 316 stainless steel substrate was sandblasted and cleaned with acetone for better laser absorption. The 17-4 PH stainless steel powder flow rate was set at constant value of 2.0 rpm (5.06 g/min)while the powder flow rate of tungsten powder was varied between 0.5 rpm to 2.0 rpm (3.15 g/min to 12. 6 g/min), The laser power, the scanning speed, the gas flow rate and the laser spot size were kept fixed at 2.6 kW, 0.5 m/s, 2.5 litres/min and 2.0 mm respectively. Table 2 presents the experimental matrix used for the deposition process.

After the 17-4 PH stainless steel-tungsten composite samples were produced, the samples were cut, mounted, grinded and polished. The samples were etched using waterless kalling`s reagent which comprises of 5 g of cupric chloride, 100 ml hydrochloric acid and 100 ml ethanol to reveal the microstructure. The microstructure of the samples was observed under optical microscopy (OM) and scanning electron microscopy (SEM) at various magnifications. Figure 1 shows the experimental set-up and the schematic diagram of the laser metal deposition process used in this research study.

Table 1. Elemental Composition of 17-4 PH Stainless Steel

Elements	**Composition (%)**
Chromium (Cr)	17.81
Nickel (Ni)	4.20
Iron (Fe)	72.26
Silicon (Si)	0.78
Copper (Cu)	3.19
Manganese (Mn)	1.27
Others	Balance

Table 2. Experimental Matrix

Sample Label	**Laser Power (kW)**	**Scanning Speed (m/s)**	**17-4 PH SS Powder flow rate**	**Tungsten Powder flow rate**	**vol.% Tungste n**	**Gas Flow Rate (l/min)**	**Spot Size (mm)**

			(rpm)[g/min]	(rpm) [g/min]			
A1	2.6	0.5	2.0 [5.06]	0.5 [3.15]	20	2.5	2
A2	2.6	0.5	2.0 [5.06]	1.0 [6.30]	33	2.5	2
A3	2.6	0.5	2.0 [5.06]	1.5 [9.45]	43	2.5	2
A4	2.6	0.5	2.0 [5.06]	2.0 [12.6]	50	2.5	2

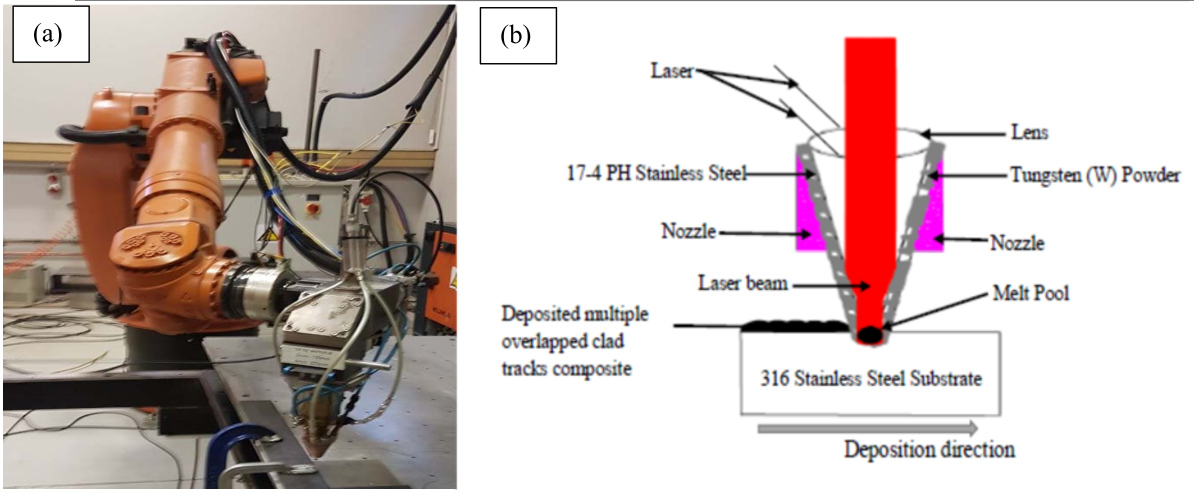

Fig.1. The (a) Experimental Set-up (b) Schematic Diagram of the LMD process [13]

3. RESULTS AND DISCUSSION

Figure 2 shows the SEM micrograph of both the 17-4 PH stainless steel powder and tungsten powder at 300 X magnification.. The 17-4 PH stainless steel powder is characterized by spherical shaped gas atomized powder. The tungsten powder is characterized by irregular shaped ball milled powder. After the samples were observed under optical microscope, it was further examined under scanning electron microscope at higher magnifications. The SEM micrographs of the multiple-track deposited composite samples are shown in Figure 3. The composite samples produced were observed under SEM and analysed at beam electron energy of 20.0 kV and at magnification range between 400 X to 1500 X.

.

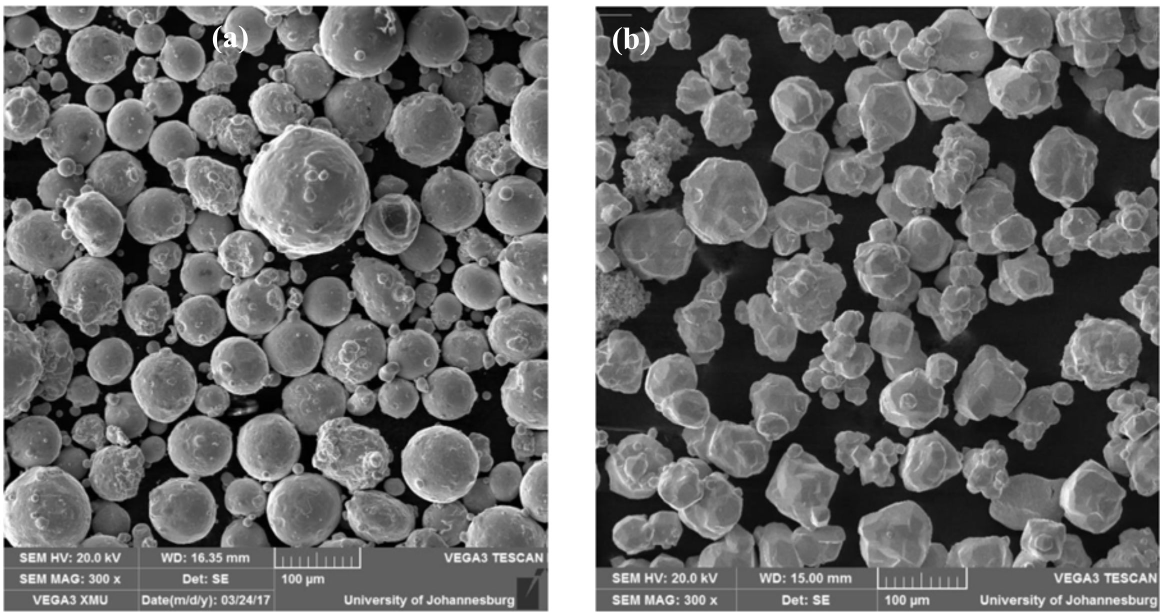

Fig.2. SEM Micrograph of (a) 17-4 PH SS powder [13] and (b) Tungsten (W) powder.

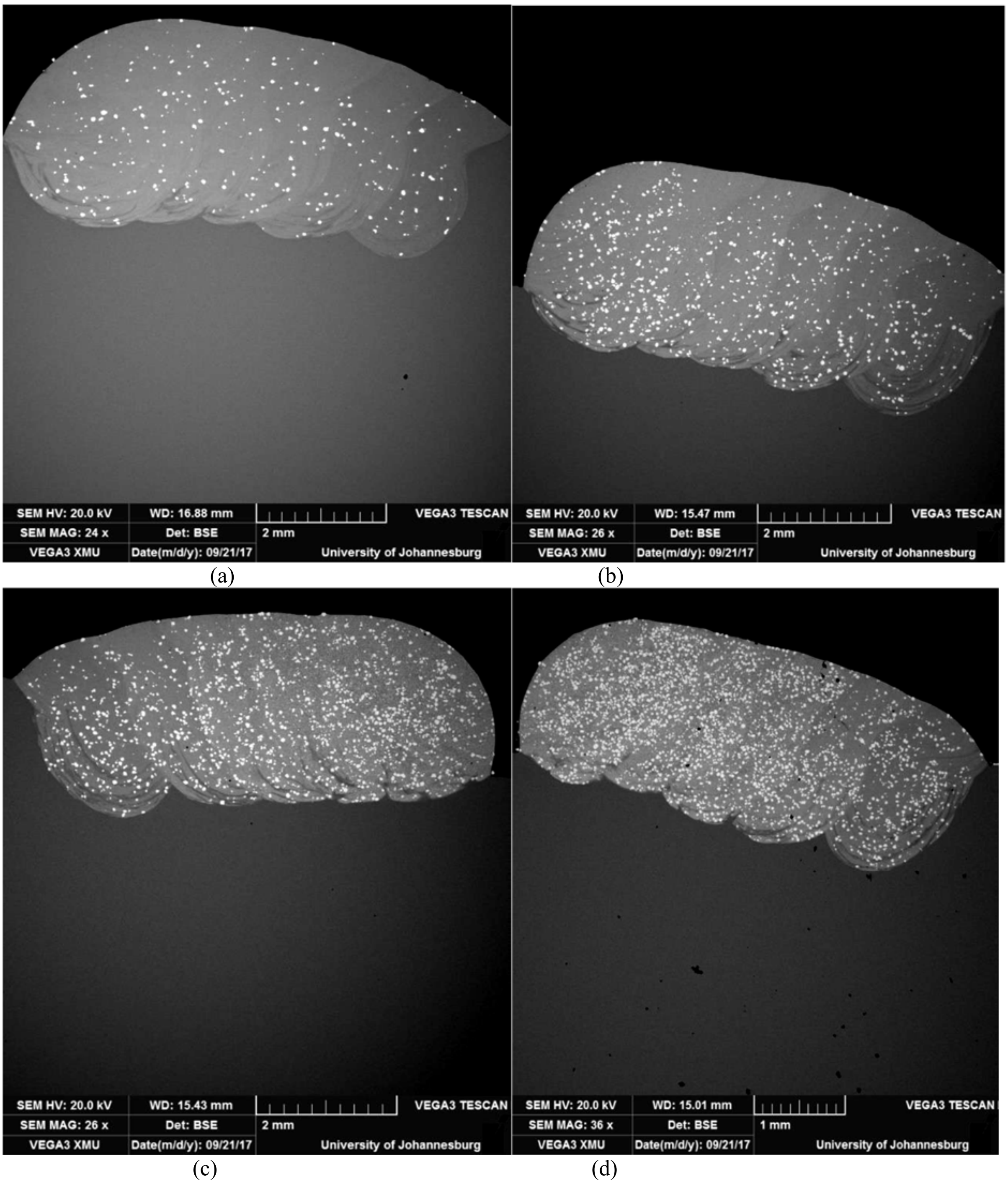

Fig.3. SEM Micrograph of multiple-track 17-4 PH SS-W composite deposited at tungsten flow rate of (a) 0.5 rpm or 20 vol.% W (b) 1.0 rpm or 33 vol. % W (c) 43 vol. % W and (d) 2.0 rpm or 50 vol. % W

The microstructure of all the composites was mostly characterized by the presence of tungsten carbide precipitates, BCC alpha (α) ferrite, FCC gamma (γ) ferrite and sigma (σ) phase precipitates. The BCC alpha (α) ferrite/FCC gamma (γ) ferrite formed will induce ferromagnetic property in the composites and also making it fairly ductile [26, 27]. All composite show discrete second-phase precipitates at the grain boundaries of the tungsten carbide precipitates. It can be observed that there are white Nano-scale precipitates that are evenly dispersed in the microstructure of the 17-4 PH SS-W composite formed. These white nano-scale precipitates were found to be tungsten carbide precipitate from EDS analysis. It was also observed that the quantity of these precipitates varies with tungsten powder flow rates or vol. % W. The quantity of tungsten carbide precipitate formed increases as the volume percent tungsten increases as shown in the SEM/EDS micrograph in Figures 4 for each composite sample. The reason for this can be attributed as more quantity of tungsten is deposited, more reaction between the carbon in the steel and the tungsten is enhanced.

Furthermore, a careful and critical observation of the microstructure through the EDS quantitative analysis shows that the amount of BCC alpha (α) ferrite and FCC gamma (γ) ferrite formed also increase as the tungsten flow rate increases. The faster solidification rate that is associated with the laser metal deposition process may have favoured this observations. Very few ferrites were seen to be formed in the microstructure at tungsten powder flow rate of 0.5 rpm (20 vol. % W). Also, few ferrites were formed in the microstructure at 1.0 rpm (33 vol. % W) and it becomes more populated in the microstructure at tungsten flow rates of 1.5 rpm (43 vol. % W) and 2.0 rpm (50 vol. % W) as shown in Figure 5. At tungsten powder flow rate of 2.0 rpm (50 vol. % W), it was observed that alpha ferrite dominated most of the areas of the microstructure. The reason of this is not farfetched, because tungsten has ferrite stabilizing effect by reacting with the carbon in the steel. With the higher tungsten content, more tungsten carbide precipitates are produced while helping to retain more ferrite. Additional observation of the microstructure of the laser deposited composite samples indicates the precipitation of sigma phase (σ) with a black dot appearance. The sigma phase (σ) is a tetragonal crystal structure which initiates embrittlement by increasing the hardness property and reduces the toughness of a stainless steel grade composite material [28, 29]. The sigma (σ) phase precipitates were observed in 17-4 PH SS-W composite sample deposited at 1.5 rpm (43 vol. % W) and 2.0 rpm (50 vol. % W) tungsten powder flow rate. The sigma (σ) phase precipitates formed appears to be more profound in the microstructure of composite deposited at high tungsten powder flow rate of 2.0 rpm (50 vol. % W). The sigma (σ) phase precipitates are normally formed in the chromium-rich region of the microstructure.

Figure 6 (a) and (b) shows the formation of the sigma (σ) phase precipitates at tungsten powder flow rate of 1.5 rpm and 2.0 rpm (43 and 50 vol. % W) respectively. This can also be attributed to the large quantity of tungsten carbide precipitated produced at high volume percentage of tungsten content in the composite couple with the rapid solidification that is associated with the laser metal deposition process.

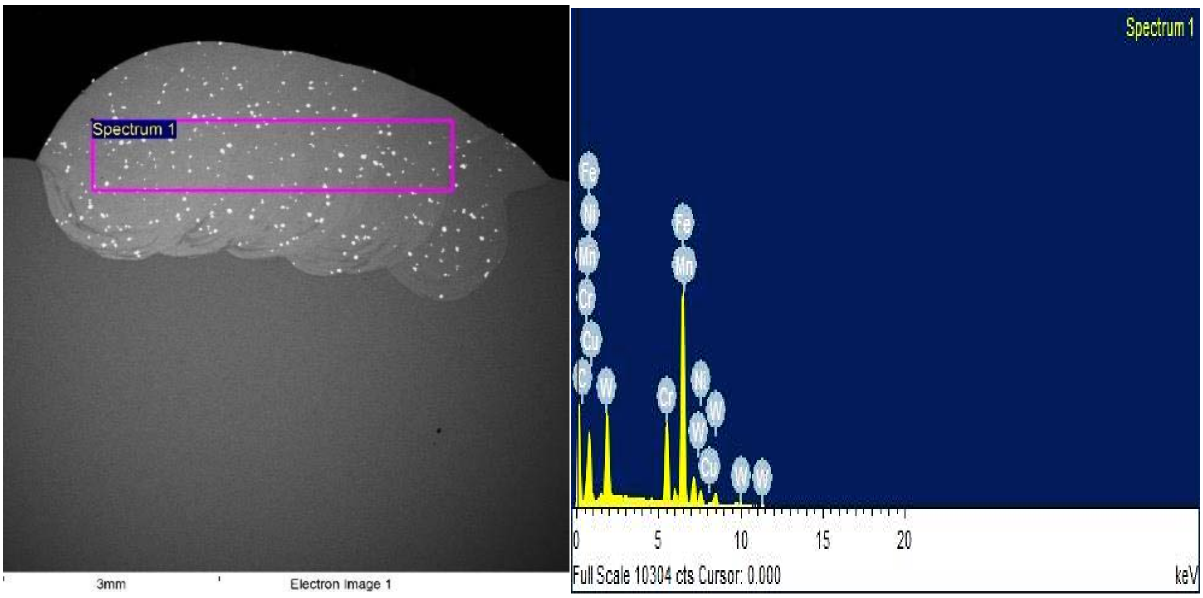

(a)

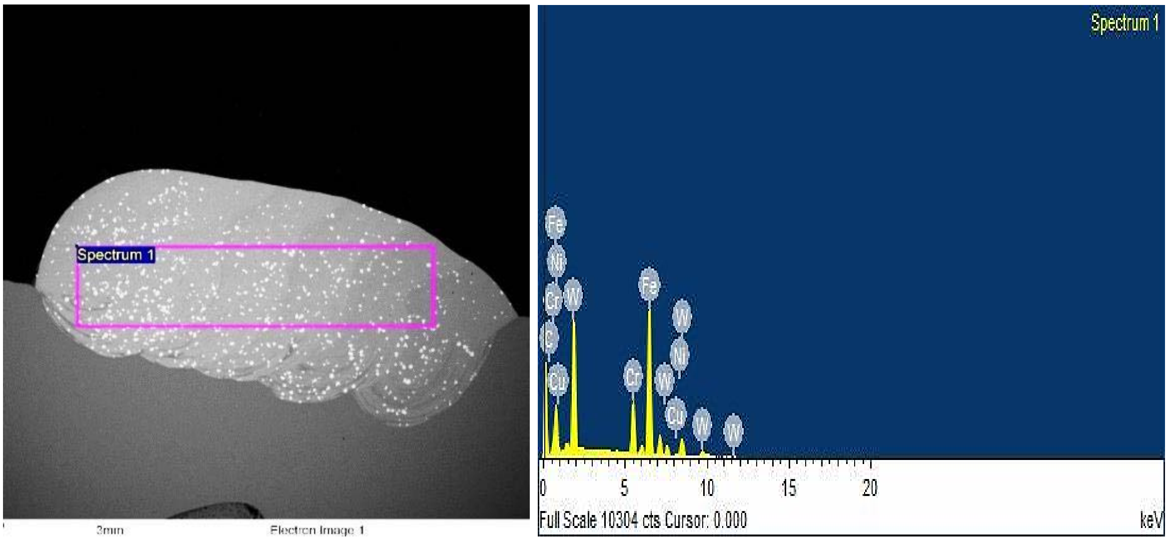

(b)

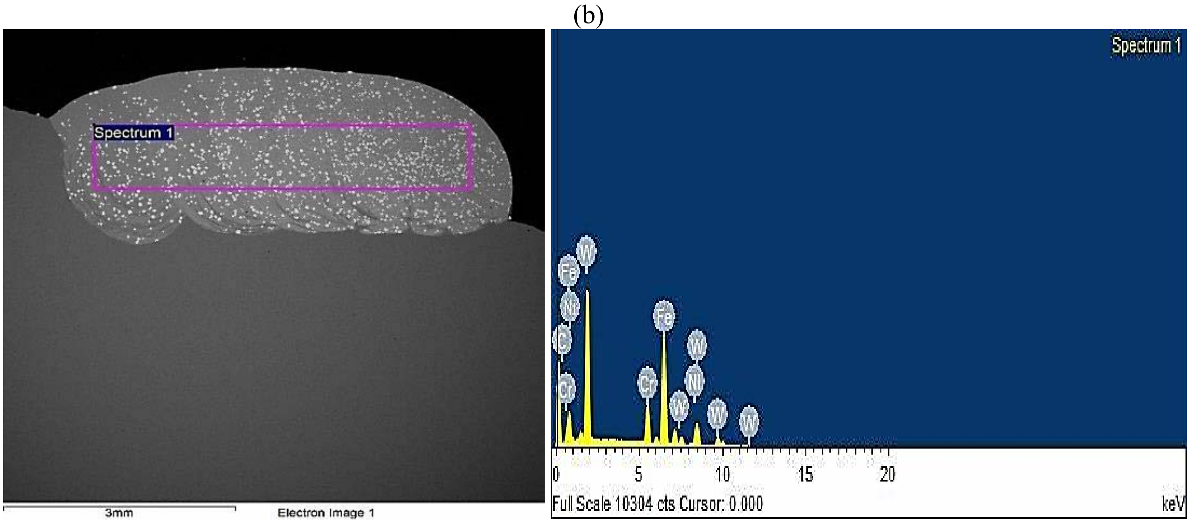

(c)

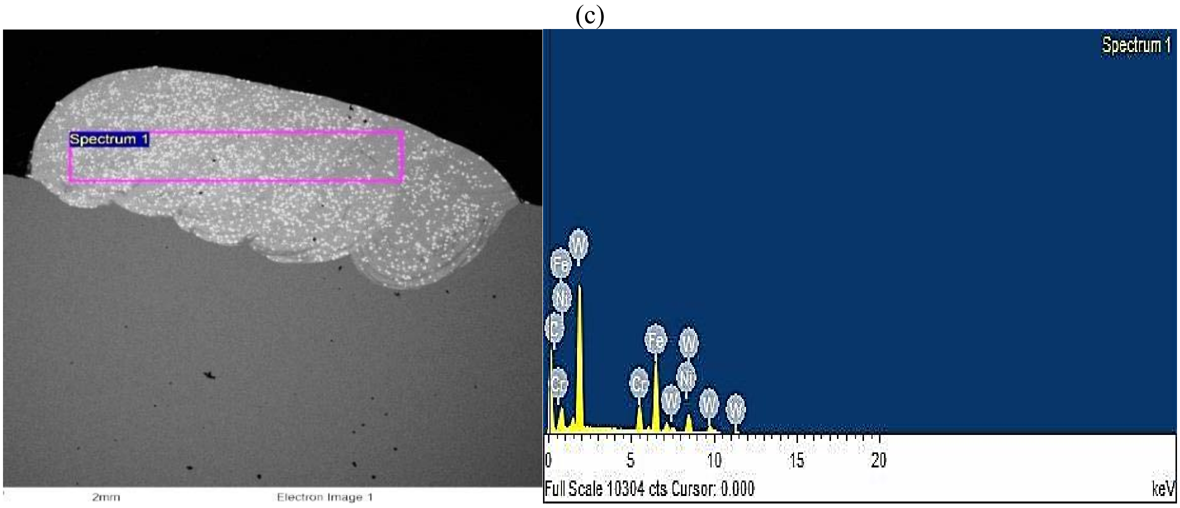

(d)

Fig.4. SEM/EDS Spectrum and analysis of Sample with (a) 20% Tungsten (b) 33 vol. % Tungsten (c) 43 vol. % Tungsten (d) 50 vol. % Tungsten

4. CONCLUSIONS

The influence of vol. % tungsten on the microstructure evolution of laser metal deposited 17-4 PH SS/W composite deposited on 316 stainless steel substrate has been studied and reported in this research work. Tungsten powder was varied between 20 and 50 vol. % ratio with 17-4 PH SS powder. Tungsten carbide precipitates were seen to be formed in all the composite samples which were found to increase with increase in volume percent tungsten. The tungsten carbide precipitates formed were observed to increase in amount simultaneously with the formation of BCC alpha (α)/FCC gamma (γ) ferrites. Sigma (σ) phase precipitates were also observed in the composite samples deposited at tungsten powder flow rates of 1.5 rpm or 43 vol. % and 2.0 rpm or 50 vol. % respectively. The presence of the sigma (σ) phase precipitate which was attributed to the larger percentage of tungsten carbide (WC) precipitates formed will promote hardness and reduce toughness. The laser metal deposited samples shows no sign of defects such as crack and pores. This study has contributed to the body of existing knowledge in that the result of this study can be used for designing novel material that can be useful in engineering application where component with tailored material properties can be produced simultaneously by using the laser metal deposition process.

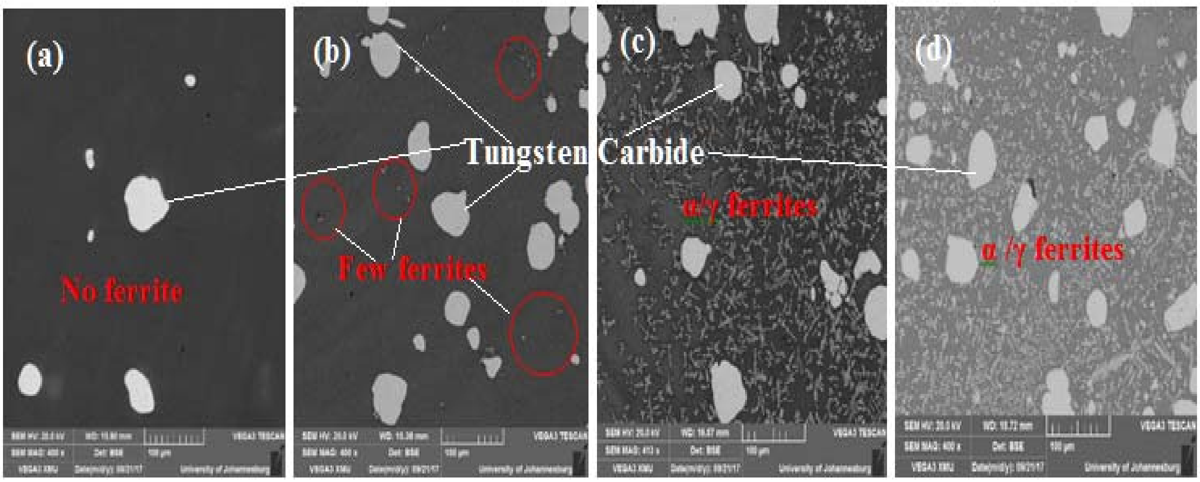

Fig.5. SEM Micrograph of ferrite formation in 17-4 PH SS-W composite at (a) 0.5 rpm and (b) 1.0 rpm (c) 1.5 rpm (d) 2.0 rpm

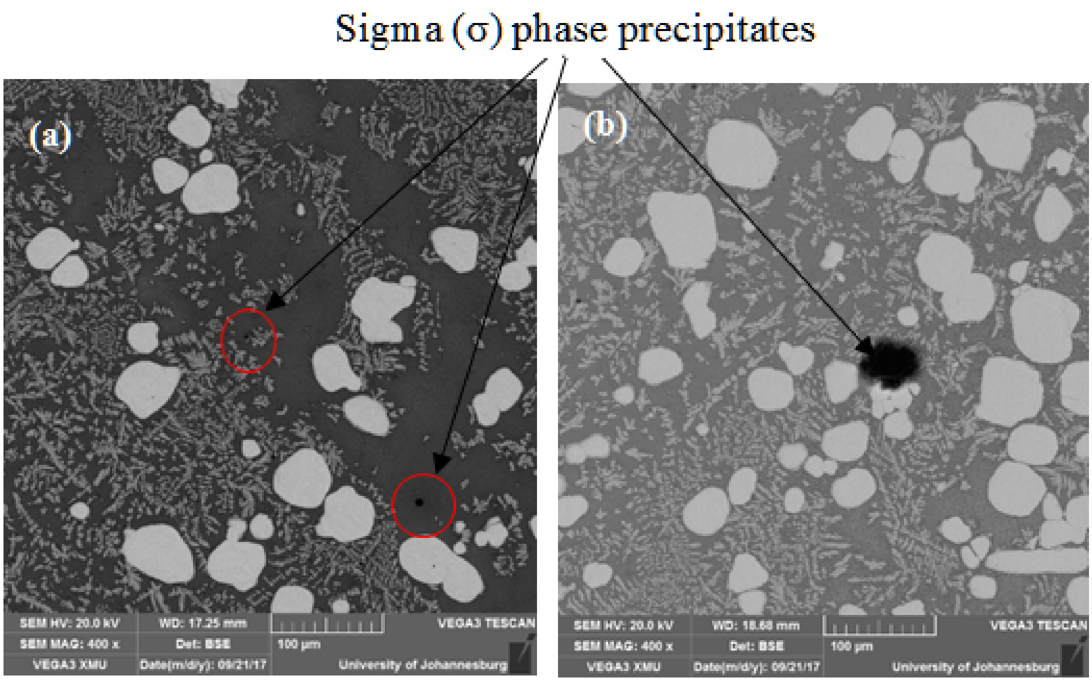

Fig.6. SEM Micrograph of sigma (σ) phase precipitates formation in 17-4 PH SS-W composite at (a) 43 vol.% Tungsten and (b) 50 vol. % Tungsten

ACKNOWLEDGEMENTS

The author acknowledges financial support of the Global Excellent and Stature (GES), University of Johannesburg and The National Laser Centre, Council for Scientific and Industrial Research (CSIR) in Pretoria, South Africa for the rental pool grant.

REFERENCES

[1] **Leslie W.C.**, *The physical metallurgy of steels*, New York: McGraw-Hill, Inc., 1981.
[2] **mith W.F.,** *Structure and Properties of Engineering Alloys*, 2nd ed., McGraw-Hill, Inc. New York, USA, pp. 328-335, 1993.
[3] **Rack H.J., Kalish, D.,** *The strength, fracture toughness, and low cycle fatigue behaviour of 17-4 PH stainless steel*, Metallurgical Transactions, 5(7), 1994, pp. 1595-1605.
[4] **Clemente R., Lepp N.W.,** *Tungsten. In Heavy Metals in Soils,* Springer Netherlands, 2013, pp. 559-564.
[5] **Ma D., Xie J., Li J., Liu S., Wang F., Zhang H., Wang W., Wang A., Sun H.,** *Synthesis and hydrogen reduction of nano-sized copper tungsten powders produced by a hydrothermal method*, International Journal of Refractory Metals and Hard Materials, 46, 2004, pp. 152-158.
[6] **Batchelor J.D., Olcott E.L.,** *Failure mechanics in dense tungsten alloy rocket nozzles*, Journal of Spacecraft and Rockets, 1(6), 1964, pp. 635-642.
[7] **Park D.Y., Oh Y.J., Kwon Y.S., Lim S.T., Park S.J.,** *Development of non-eroding rocket nozzle throat for ultra-high temperature environment*, International Journal of Refractory Metals and Hard Materials, 42, 2014, pp. 205-214.
[8] **Mahamood R.M.,** *Laser Metal Deposition Process of Metals, Alloys, and Composite Materials*, Springer, Switzerland, 2018.
[9] D. Shabat1, Y. Rosenthal1, D. Ashkenazi, A. Stern, Mechanical and Structural Characteristics of Fused Deposition Modelling ABS Material. Annals of "Dunarea de Jos" University, Fascicle XII, Welding Equipment and Technology, 28, 2017, pp. 16-24
[10] **Rosenthal, Y. Sharon, A. Stern,** Multi-Material Processing: Hybrid Disk-Shaped Parts Wrought AA6061 & AM-SLM AlSi10Mg. Annals of "Dunarea de Jos" University, Fascicle XII, Welding Equipment and Technology, 28, 2017, pp. 5-10.
[11] **Berger A., Sharon Y., Ashkenazi D., Stern A.,** Test artifact for additive manufacturing technology: FDM and SLM preliminary results, The Annals of "Dunarea De Jos" University of Galati Fascicle XII, Welding Equipment and Technology 27, 2016, pp. 29–37.
[12] **I. Rosenthal, A. Stern,** Heat Treatment Investigation of the AlSi10Mg Alloy Produced by Selective Laser Melting (SLM): Microstructure and Hardness, The Annals of "Dunarea De Jos" University of Galati Fascicle XII, Welding Equipment and Technology 27, 2016, pp. 7–11.
[13] **Adeyemi A. A., Akinlabi E.T., Mahamood R. M.,** Influence of Laser power on Microhardness and Wear Resistance Properties of Laser Metal Deposited 17-4 PH Stainless Steel. *Annals of "Dunarea de Jos" University of Galati, Fascicle XII, Welding Equipment and Technology*. 2018, Accepted
[14] **Gu D. D., Meiners W., Wissenbach K., Poprawe R.,** *Laser additive manufacturing of metallic components: materials, processes and mechanisms*, Intl. Mat. Reviews, 57(3), 2012, pp.133-164.
[15] **Wang Z., Palmer T. A., Beese A. M.,** *Effect of processing parameters on microstructure and tensile properties of austenitic stainless steel 304L made by directed energy deposition additive manufacturing*, Acta Materialia, vol. 110, 2016, pp. 226 – 235.
[16] **Mahamood R. M., Akinlabi E. T., Shukla M. and Pityana S.,** *Effect of processing parameters on properties of laser metal deposited Ti6Al4V using design of experiment*, IAENG Transactions on Engineering Sciences, Taylor & Francis Group, London, ISBN 978-1-138-00136-7, 2014, pp. 331-339.
[17] **Bayode A., Akinlabi E. T., Pityana S.,** *Characterization of Laser Metal deposited 316L Stainless Steel*, Proceedings of the World Congress on Engineering, vol. 2, ISSN: 2078-0958 (Print); ISSN: 2078-0966 (Online), 2016.
[18] **Bayode A., Akinlabi E. T., Pityana S.,** *Microstructure and Microhardness of 17-4 PH Stainless Steel Made by Laser Metal Deposition.* Proceedings of the World Congress on Engineering, vol. II, ISBN: 978-988-14048-2-4, 2016.
[19] **Adeyemi A. A., Akinlabi E. T., Mahamood R. M., Sanusi K. O., Pityana S., Tlotleng, M.,** *Influence of laser power on microstructure of laser metal deposited 17-4 PH stainless steel*, IOP Conference Series: Materials Science and Engineering, vol. 225, no. 1, pp. 012028., 2017.
[20] S. Pityana, R. M. Mahamood, E. T. Akinlabi, and M. Shukla, (2013). Effect of gas Flow Rate and powder flow rate on Properties of Laser Metal Deposited Ti6Al4V. 2013 International Multi-conference of Engineering and Computer Science (IMECS 2013), March 2013. 848-851.
[21] M. Shukla, R. M. Mahamood, E. T. Akinlabi and S. Pityana, (2012). Effect of Laser Power and Powder Flow Rate on Properties of Laser Metal Deposited Ti6Al4V. World Academy of Science and Technology, vol.6, 44-48.
[22] **Mahamood R. M., Akinlabi E. T., Shukla M. and Pityana S.,** *Scanning velocity influence on microstructure, microhardness and wear resistance performance of laser deposited Ti6Al4V/TiC composite*, Materials and Design, vol. 50, 2013, pp. 656–666.
[23] **Mahamood R. M., Akinlabi E. T., Shukla M., Pityana S.,** *Characterization of Laser Deposited Ti6A14V/TiC Composite Powders on a Ti6A14V Substrate*, Lasers in Engineering, vol. 29, 2014, pp. 197-213.
[24] **Popoola A. P., Pityana S., Ogunmuyiwa E.,** *Microstructure and wear behaviour of Al/TiB2 metal matrix composite*, Advanced Materials Research, 2011, pp. 23-26.
[25] R.M. Mahamood, E.T. Akinlabi, (2015), Effect of Processing Parameters on Wear Resistance Property of Laser Material Deposited Titanium -Alloy Composite, Journal of Optoelectronics and Advanced Materials (JOAM), Vol. 17, No. 9-10, Pp. 1348 - 1360.
[26] **Bhadeshia, H., Honeycombe, R.** *Steels: Microstructure and Properties*, Butterworth-Heinemann, 2011.
[27] **Maranian P.,** *Reducing Brittle and Fatigue Failures in Steel Structures*, American Society of Civil Engineers, ISBN 978-0-7844-1067-7, 2009.
[28] **Duhaj P., Ivan J., Makovicky E.,** *Sigma phase precipitation in austenitic steels*, The Journal of the Iron and Steel Institute, vol. 206, 1968, pp. 1245–1252.
[29] **Souza C. M., Abreu H. F. G., Tavares S. S. M., Rebello J. M. A.,** *The σ phase formation in annealed UNS S31803 duplex stainless steel: texture aspects*, Materials Characterization, vol. 59, no. 9, 2008, pp. 1301–1306. .
.